

## **Spray Cooling Processes for Space Applications**

**John P. Kizito\*, Randy L. Vander Wal, Gordon Berger**

National Center for Microgravity Research, NASA Glenn Research Center, 21000 Brookpark Rd, Cleveland, OH 44135

\*Tel 216 433 2275, Fax 216 433 3793, John.Kizito@grc.nasa.gov

and

**Gretar Tryggvason**

Worcester Polytechnic Institute

### **Abstract**

The present paper reports ongoing work to develop numerical and modeling tools used to design efficient and effective spray cooling processes and to determine characteristic non-dimensional parametric dependence for practical fluids and conditions. In particular, we present data that will delineate conditions towards control of the impingement dynamics of droplets upon a heated substrate germane to practical situations.

### **INTRODUCTION**

Current data on droplet dynamics is scarce for the sizes and velocities typical of practical applications. In particular, improved understanding of drop breakup dynamics is needed to optimize the desired behavior of impinging drops in practical situations such as spray combustion in diesel engines, rocket engines, agricultural and medical sprays, spray painting, printed circuit manufacturing, aircraft icing and spray cooling of high heat-flux electronic components.

While much more representative of practical applications, the small spatial scales and rapid time-scales prevent detailed measurement of the internal fluid dynamics and liquid property gradients produced by impinging upon surfaces. Realized through the extended spatial and temporal scales afforded by a microgravity environment, an improved understanding of drop breakup dynamics is sought to understand and ultimately control the impingement dynamics of droplets upon surfaces in spray cooling.

Our long term goal is to investigate the mechanism(s) for droplet breakup and the effects of relative droplet-surface temperature, ambient pressure and impingement angle on spray cooling processes. Furthermore, we are developing numerical models that are benchmarked against experimental data capable of predicting droplet-wall dynamics. In practical applications, droplet sizes range from 10 - 100 microns with velocities extending from 1 to beyond 10 m/s. These small spatial scales and short temporal scales prohibit detailed study of the internal fluid dynamics and temperature profiles during droplet-wall interaction.

In the past, direct numerical simulations applying the full Navier-Stokes equations to problems that contain free interfaces which are highly deformable have been difficult and computationally time consuming. To this end, a number of investigators have produced numerical results involving droplet-wall interactions with small parameters far below the

splashing threshold. Therefore, the primary objectives of this paper is to report ongoing work on numerical, experimental, and modeling tools used to investigate the physical mechanism leading to different “splashing modes” and to determine how that process influences spray cooling.

The complete droplet and heated wall interaction problem is highly dependent on the simultaneous coupling of many effects none of which can typically be ignored. The modeling of mass, momentum and energy transport must include surface tension [1], discontinuous material properties and complicated liquid-vapor interface dynamics. We use a two-dimensional axisymmetric front-tracking finite difference code for fluid flow that enables the simulation of problems involving complex motion of the large interface deformations and topology changes with or without a temperature field. The method is based on a finite difference approximation of the Navier-Stokes and energy equations on an unmoving, structured grid and an explicit tracking of the liquid interface on a moving, unstructured grid. The method is an extension of techniques already developed for isothermal, multifluid flows without phase change in both two and three dimensions by Unverdi and Tryggvason [2]. The multifluid code has also been used to investigate the collision of drops, thermal migration of drops and the motion of clouds of bubbles [3,4,5].

## THEORETICAL CONSIDERATIONS

### Formulation and Numerical Method

Consider a domain consisting of a fluid droplet as shown in **Figure 1**.

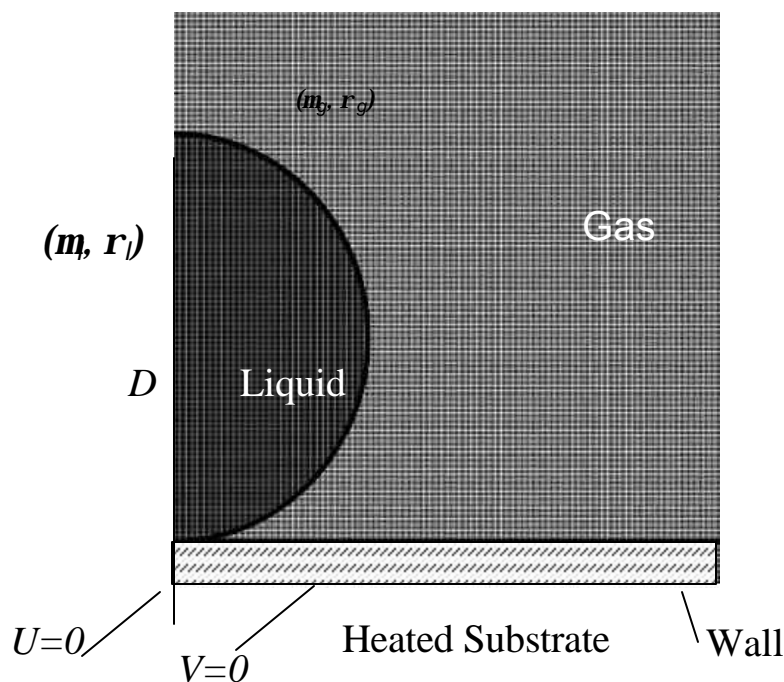


**Figure 1** Schematic illustration of computational domain and boundary conditions.

For simplicity, let the material properties of the phases be constant but different within each phase. The basic equations that describe the laws of conservation of mass, momentum, and energy for each phase and jump conditions across the interface are given below. The equations

are solved using the front tracking method where the equations of motion are discretized by the finite difference method on a Cartesian non-uniform staggered mesh. Our approach involves treating the liquid boundary surface as an imbedded interface by adding the appropriate source terms to the conservation laws (momentum, energy and mass). These source terms are in the form of delta functions localized at the interface and are selected in such a way so as to satisfy the correct matching conditions at the phase boundary.

### Scaling Analysis

The momentum equation can be non-dimensionalized and normalized to give parameters which describe the process. We normalize the momentum equation by dividing through by the inertia term. The resulting equation will contain the following parameters: Reynolds number,  $Re$ , Weber number,  $We$ , Peclet number,  $Pe$ , density, thermal conductivity, aspect and viscosity ratios described as:

$$Re = \frac{\mathbf{r}UD}{\mathbf{m}}, \quad We = \frac{\mathbf{r}U^2D}{\mathbf{s}}, \quad Pe = \frac{\mathbf{r}c_pUD}{k}, \quad \frac{\mathbf{r}_l}{\mathbf{r}_g}, \frac{k_l}{k_g}, \frac{c_{pl}}{c_{pg}}, \frac{D}{L} \text{ and } \frac{\mathbf{m}_l}{\mathbf{m}_g}.$$

The characteristic time is given as  $T_R$  seconds:  $T_R = \frac{D}{U}$

Where,  $D$  is the diameter of the initially spherical drop,  $L$  is the domain size and  $U$  is the impact velocity. The temperature is scaled by the maximum difference. For the example presented here, a drop diameter  $D = 0.00196$  m, impact velocity  $U = 2.17$  m/s, and  $T_R = 0.0009$  seconds. The temperature difference was held at 10 degrees for all simulated cases ( $\Delta T = 10$ ).

**Table 1.** Ethanol Property Parameters

Thermal capacity cp J/(kg K)	Thermal conductivity k W/(m K)	Surface tension $\sigma$ (N/m)	Density (mass) $\rho$ kg/m <sup>3</sup>	Dynamic viscosity $\mu \cdot 10^6$ Pa.s
2840	0.18	0.023	789.3	1200

**Table 2.** Representative Non-Dimensional Parameters

$Re$	$We$	$Pe$	$\frac{\mathbf{r}_l}{\mathbf{r}_g}$	$\frac{k_l}{k_g}$	$\frac{c_{pl}}{c_{pg}}$	$\frac{D}{L}$	$\frac{\mathbf{m}_l}{\mathbf{m}_g}$
2824.	317.8	53201.	681	6.92	2.82	0.25	64.9

### Numerical Test Matrix

Table 3 summarizes the parameters used for the numerical simulation cases.

**Table 3.** Numerical Parameters for the simulated experiments

Case	$Re$	$We$	$Pe$	$k$ ratio	$\mathbf{m}$ ratio	$\mathbf{r}$ ratio
1	2777.8	316.9	53201	6.92	64.9	681
5	27.8	3.17	50	2	25.7	10
9	277.8	31.7	5	200	257.	10
11	277.8	316.9	500	2	257.	10

### Problem definition

Axisymmetric representation permits simulation of half of the domain as shown in **Figure 1**. The initial height of the liquid film is of the same order of magnitude as the diameter of the drop. The drop diameter  $D$  at a velocity  $U$  approaches a substrate at temperature  $T_b$ . The subscript  $l$  represents the liquid and  $g$  represents the gaseous phase. We assume a no slip and no penetration boundary condition at the wall. We have found that a grid size of 400x400 is adequate to capture the physics.

### EXPERIMENTAL METHODS

Figure 2 illustrates our basic experimental approach. A Kodak EktaPro HG 2000 high-speed camera was manually triggered and recorded the droplet impact at 2000 frames/sec for half of the imaging field. The exposure time was set at 28 ms while using a 105 mm Nikkor lens set at an aperture of 32 to minimize motion blurring and to provide a large depth of field. A halogen lamp illuminated the impact site through a single sheet of Roscoe 111 diffusion film to provide uniform high intensity back lighting. An Incandescent lamp was used to provide back-illumination. A droplet deployment device was positioned above a heated billet. The inertial-based release mechanism included interchangeable needles to hold different volumes of a wide variety of liquids with many different physical properties. Droplets were measured volumetrically and manually placed on the needle with a syringe. A droplet size of 0.197 cm in diameter (4  $\mu$ L volume) was chosen because the liquid maintained a spherical shape throughout the free fall, negating concerns of an uneven impact. The liquid was then deployed by way of a simple manual trigger that released a rubber band in tension at the top of the mechanism. The relaxing rubber band then moved the needle quickly upward, pulling it out of the liquid droplet and releasing the droplet to fall onto the film below.

Droplet velocities were increased or decreased by translating the release mechanism vertically and taking advantage of gravitational acceleration. All velocities were measured using XCAP 2.0, an image acquisition and analysis program from EPIX. Measured velocities have an error of  $\pm 0.15$  m/s based on the pixel size and 0.5 ms image spacing.

The temperature of the heated billet is held constant during the droplet impact. Visualization of the droplet-wall interaction is achieved through a combination of high speed video and repetitive stop action photography whereby images at different stages of evolution are captured from separate but equivalent events.

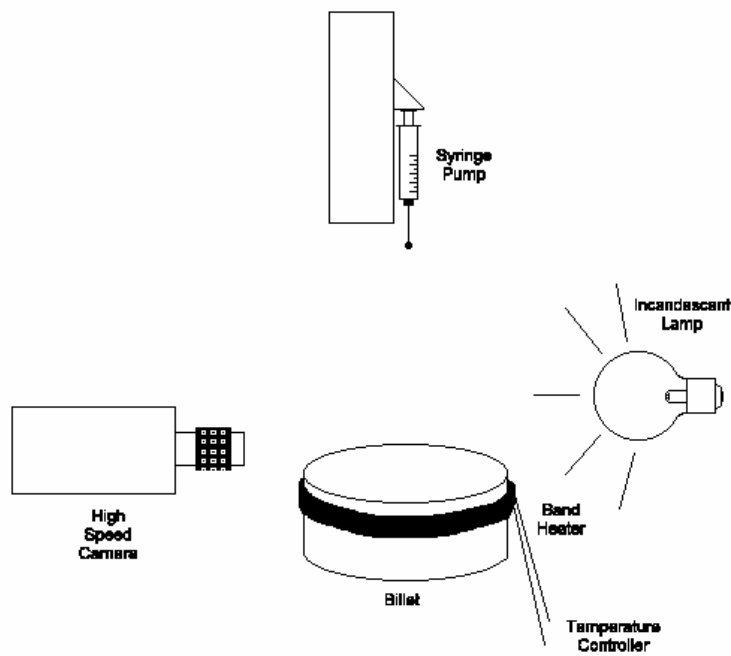
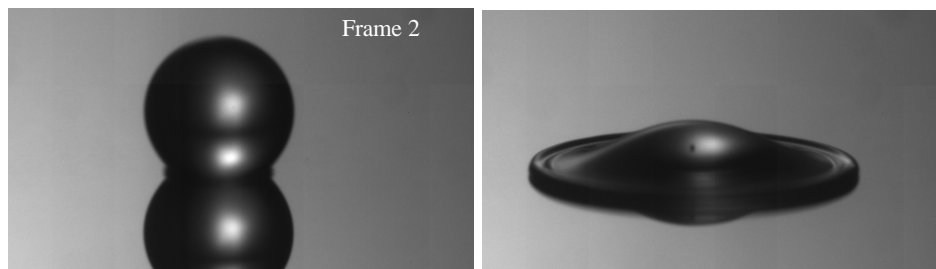


**Figure 2** Schematic illustration of experimental setup.

The fluids used include alkanes (HPLC grade heptane and hexadecane and anhydrous decane) and alcohols (spectrophotometric grade methanol and n-propanol and reagent grade butanol), whose properties were gathered experimentally. Deionized water was obtained from a Millipore AFS filtration system. The properties of the glycerol solution were measured using a Cannon-Fenske (Reverse Flow) viscometer and Cahn tensiometer. Table 1 contains relevant properties of a sample fluid used in this study.

## RESULTS

An example of our experimental data is presented below in Figures 3. These images are of a relatively high viscosity fluid ( $Re=620$ , and  $We=104$ ), hexadecane impacting a mirror-polished surface. At a higher impact velocity,  $3.15\text{m/s}$  ( $Re=1436$ , and  $We=559$ ), the droplet forms splashed products.



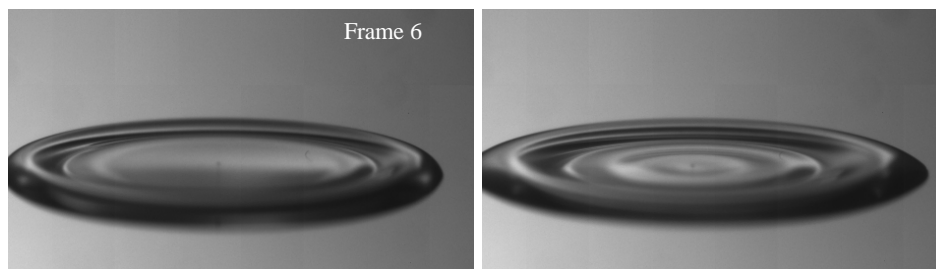


Figure 3. Hexadecane impacting a mirror-polished surface at 1.36m/s ( $Re=620$ , and  $We=104$ ). The images were acquired using a high-speed camera at 2000 frames per second.

The droplet interaction with a heated substrate was computed for a variety of parameters listed in table 1. The computational domain was 4 times the droplet diameter in each direction and was resolved by a grid of 400x400 nodes (the results were independent of the grid size). The computational results are shown in Figure 4 and denoted by case number. Figure 4 shows numerical simulations of a droplet-wall interaction.

Figure 4 shows results of collision of cold droplet with a heated substrate at dimensionless time,  $t = 20$  for the parameters listed in Table 3. The isotherms are shown on the left and the corresponding velocity vector map is shown on the right. These cases show the effect of viscosity, surface tension, and thermal diffusivity represented by  $Re$ ,  $We$ , and  $Pe$  respectively. Other parameters that represent the fluid property ratios were varied. The parameters were changed by an order of magnitude to determine the mechanism that allows maximum heat transfer between a cold droplet and a heated wall. The assessment is mostly qualitative; determined by the extent of spreading and the concentration of isotherms next to the heated substrate (thermal boundary layer formation). The concentration of isotherms indicates increased thermal energy transport to the droplet.

For all cases, the motion of the droplet draws cold gas towards the heated substrate. As the droplet approaches the heated wall, it displaces the ambient gas from the substrate depending on the control parameter. The droplet will come into contact with the wall and then deform interchanging the energy between kinetic and surface energies. Depending on the magnitude of the initial kinetic energy and the exchange dynamics between kinetic and surface energy, the droplet will either rebound or remain in contact with the surface. The effect of surface tension is to minimize surface area. When kinetic energy reaches a minimum, a surface tension force causes the flattened droplet to retract to its former spherical shape thus causing the droplet to rebound and leave the substrate. The amount of heat transferred depends on the interaction time and the extent of droplet spread.

Let's use case 1 as the basis of comparison for all numerical simulation data in Figure 4. The parameters for case 1 were exactly matched with the experimental parameters shown in table 2. Numerical experiments show that the density ratio is not sensitive to the droplet shape. The isotherms shown in case 1 are closer to each other because of the high  $Pe$  number. The isotherms shown in case 1 are closer to each other because of the high  $Pe$  number. The effect of increasing the impact velocity is apparent when case 1 is compared with case 5. At low impact velocity, the droplet remains spherical and hardly displaces any air from the heated substrate. In addition, the heat transfer in case 5 is poor because of minimal interaction with the substrate. The effect of low  $We$  number is evident in case 9. The droplet undergoes a small deformation

which leads to a shortened droplet-wall interaction time and a much quicker rebound. The shorter stay at the heated wall will result in diminished cooling effect by the droplet.

The effect of increasing the fluid viscosity is demonstrated by case 11. Here, the  $Re$  number is reduced while the  $We$  number is held constant. The spread extent decreases and the droplet deforms to a disc-like shape. This case provides for the best heat transfer profile because of increased surface area of the fluid in contact with the heated substrate. In addition, the center of the droplet is not drained of its liquid, consequently there is more fluid heat capacity available.

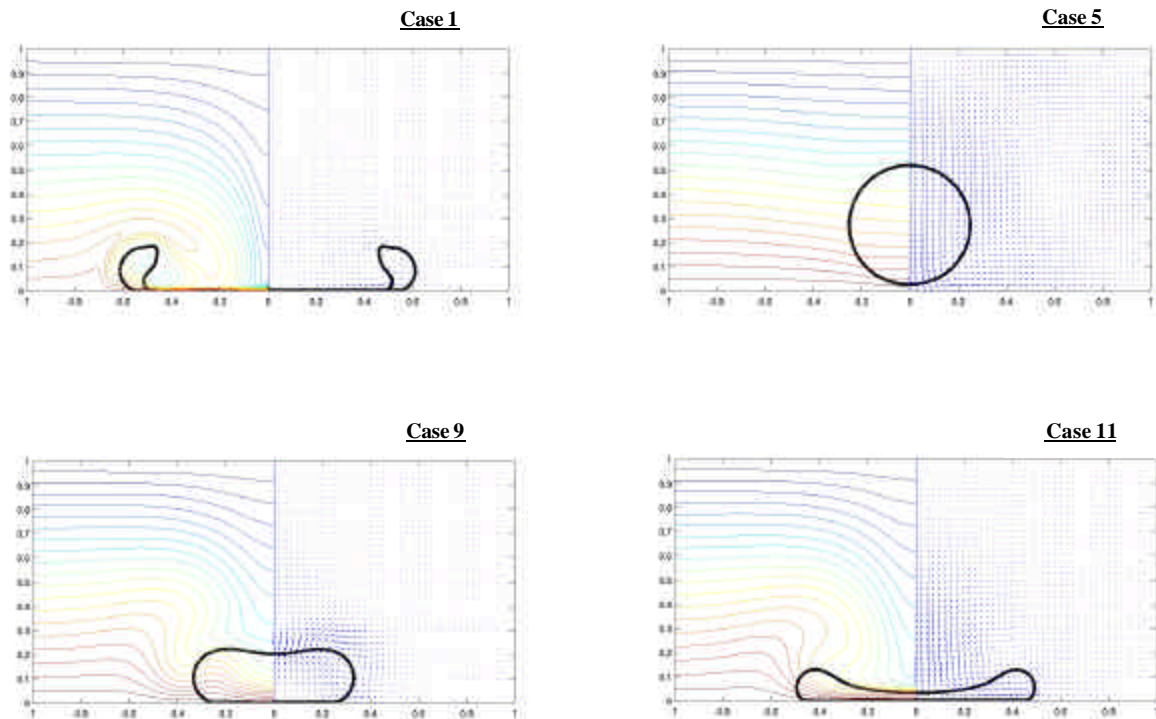


Figure 4. Collision of a cold droplet with a heated substrate at dimensionless time,  $t = 20$  for the parameters list in Table 3. The isotherms are shown on the left and the corresponding velocity vector map is shown on the right.

## CONCLUSIONS

We have presented numerical and experimental data used to investigate the physical mechanism leading to “splashing modes” and to determine parametric non-dimensional number dependencies for impinging droplets on spray cooling. The data shows that for non-evaporating drop approaching and interacting with a heated substrate, maximum heat is transferred when the droplet has the widest extent of spread on the substrate and does not form a crown or splashed

products. Therefore, it is important to know and map splash regimes in order to design effective droplet cooling devices.

### **ACKNOWLEDGEMENTS**

This work was supported by a NASA NRA 98-HEDs-03 fluid physics award administered through NASA cooperative agreement NCC3-975 with The National Center for Microgravity Research on Fluids and Combustion (NCFM) at The NASA-Glenn Research Center. The authors gratefully acknowledge Steven D. Mozes and Premal D. Patel for assistance with the experiments. Also, we are grateful to Dr Asghar Esmaeeli for assistance with the numerical code.

### **REFERENCES**

1. Gupta N. R., Balasubramaniam R. and Stebe K. J. (2002) "Rapidly Expanding Viscous Drop from a Submerged Orifice at Finite Reynolds Numbers", Ann. New York Academy Sci. An. N.Y. Acad. Sci. 974:398-409
2. Unverdi, S. O. and Tryggvason, G. (1992) "A front-tracking method for viscous, incompressible", multi-fluid flows. J. Comp. Phys. 100: 25-37
3. Nobari, M. R., Jan, Y.J., and Tryggvason, G. (1996) "Head on collision of drops - numerical investigation", Phys. Fluids 8, 29-42.
4. Nas, S. and Tryggvason, G. (1993) "Computational investigation of thermal migration of bubbles and drops", In Fluid Mechanics Phenomena in Microgravity, AMD 174/FED 175, pp. 71-83. ASME: New York.
5. Esmaeeli, A. and Tryggvason, G. (1996) "An inverse energy cascade in 2-dimensional low Reynolds number bubbly flows", J. Fluid Mech. 314: 315-330.